A numerical and analytical study on the role of geogrid reinforcement in veneer stability

A. Lavasan. Huesker Synthetic GmbH, Gescher, Germany. lavasan@huesker.de
L. Carbone. Huesker Synthetic GmbH, Gescher, Germany. carbone@huesker.de
P. J. Assinder. Huesker Synthetic GmbH, Gescher, Germany. assinder@huesker.com

ABSTRACT
Landfill covers and basal barriers typically consist of multi-layers, often with combinations of geosynthetic and soil layers. Smooth and textured geomembranes are used in such structures to provide part of a composite sealing system. Tensile load is transferred to the geosynthetic layers over the design life of the landfill barrier and particular attention should be paid to avoid the development of excessive tensile loads within the geomembrane.
The role of the geogrid in two different geocomposite liner configurations is studied numerically and analytically by maintaining strain compatibility and force equilibrium within the lining system. The influence of the reduction of interface shear strength and the tensile forces transferred into the geosynthetic are also presented.
It is demonstrated that the use of appropriate geogrid reinforcement plays a decisive role to guarantee both the stability of the entire system and to limit the tensile loads and strains within the geomembrane.

1. INTRODUCTION

Modern landfills are multi-barrier systems composed of different layers of mineral materials, namely different types of soil, or of soil-geosynthetic composite systems. In order to optimise the volume of waste, it is common practice to construct lateral barriers and cover systems as steep slopes. The overall stability of a landfill is linked to the stability of the liner systems.
In designing a landfill cover it should first guarantee the stability of the system on the slope (i.e., global stability of the slope, internal stability of the cover soil layer, stability of the component parts at the interfaces). Another important aspect that it is often overlooked is the possible tensile load transfer within and between the individual geosynthetics.

Geosynthetics placed on side slopes of a landfill can experience tension during construction of the liner system, (i.e., wind up-lift on uncovered areas, movement of heavy vehicles and frictional forces from the cover soil) (Thusyanthan et al., 2007). Following closure of a landfill, the continued settlement of the waste within the cell can create down-drag (Jones and Dixon, 2005). Consequently, the interaction of the interfaces can change over time and can result, for example, in a reduction of the interface friction angle, which may induce tension in the geosynthetic layers. When tension is developed the friction angle at the contact zone can play a critical role. Results of former studies (Frost and Lee, 2001; Hebeler et al., 2005¸ Stark et al. 1996) indicate that the interface friction angle can reduce from its peak value to the residual friction angle. Lower interface friction angles can provide less shear resistance at the contact which can lead to higher tensile force in the geocomposite liner. It is important to calculate these tensile loads in order to assure adequate long-term performance, especially in relation to geomembranes, which are not designed to be subjected to unforeseen tensile loads (Thusyanthan et al., 2007).

The use of geomembranes in landfill liners for sealing purposes is a well-established technology. Two main types of geomembranes are used: smooth geomembranes and textured geomembranes. One of the main important aspects to be considered, regarding geomembrane serviceability, is to avoid stress transfer, which can induce stress cracking within the geomembrane (Rowe, 2005).

This study investigates the tensile loads transferred into the geosynthetic layers assuming that in-situ deformations mobilize the residual interface friction angle as the critical case.

Since the calculation of tensile load transfer into the system is very complex, numerical analysis methods can be employed. Liu and Gilbert, (2005) proposed graphical solutions based on a simple analytical model (Liu and Gilbert, 2003) that maintains strain compatibility and force equilibrium of the system
In this paper, the assessment of geosynthetic tension forces induced in two different geocomposite liner configurations, including a smooth geomembrane and a double-sided textured geomembrane, is carried out by applying Liu and Gilbert's (2005) method and further validated by finite element numerical analysis. The role of geogrid reinforcement in the geocomposite liner is also investigated.

2. DESCRIPTION OF THE SYSTEM AND ASSUMPTIONS

2.1 Characteristics of the gecomposite liners

The geocomposite liner considered in this study is 30 m long, with a slope inclination β equal to 15°. The liner comprises the following interfaces from top to bottom (Figure1):

- Granular soil layer
- Geogrid (solution A only)
- Geotextile
- Geomembrane (smooth for Solution A and double textured for Solution B)
- Clay

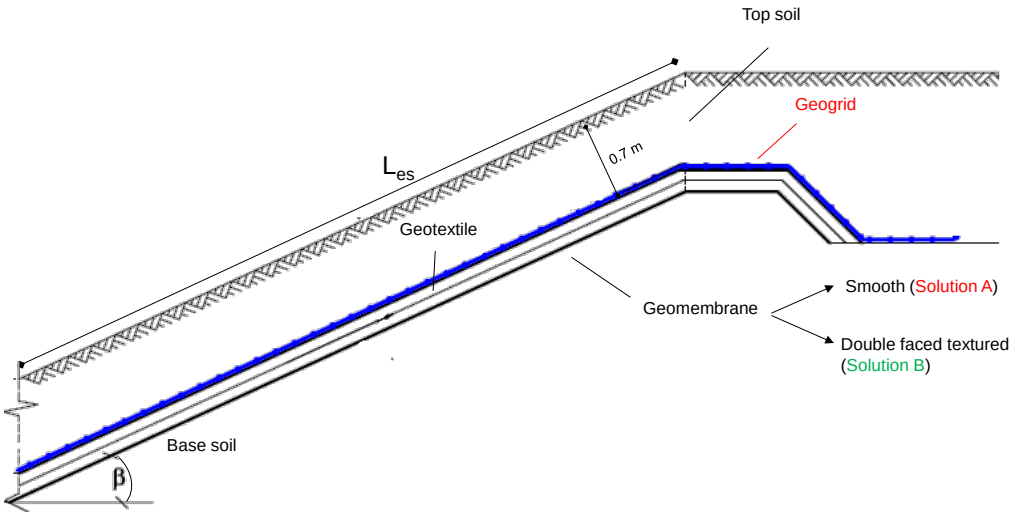

Figure 1. Scheme of the geocomposite liners considered in the study.

The main characteristics of the materials and the interface friction angles are summarized in Table 1. In solution A the liner system includes a smooth geomembrane and a geogrid, whilst in solution B a double sided textured geomembrane is considered.

Table 1. Characteristics of the geocomposite liners considered in the study.

Material	**Solution A**		**Solution B**	
	Properties	Interface friction angles	Properties	Interface friction angles
Granular soil	γ_{soil}= 18 kN/m^3 ϕ_{soil} = 32° t_{soil} = 0.7m K_c= 485 kN/m	$\phi_{soil/GTX}$ = 29°	γ_{soil}= 18 kN/m^3 ϕ_{soil} = 32° t_{soil} = 0.7m K_c= 485 kN/m	$\phi_{soil/GTX}$ = 29°
Geotextile (GTX)	$K_{t,GTX}$= 23.83 kN/m	$\phi_{GTX/GMB}$ = 16°	$K_{t,GTX}$= 23.83 kN/m	$\phi_{GTX/GMB}$ = 31°
Geomembrane (GMB)	$K_{t,GMB}$= 248 kN/m	$\phi_{GMBs/clay}$ = 13° (peak value) $\phi_{GMBs/clay}$ = 11° (residual value)	$K_{t,GMBt}$ = 232.5 KN/m	$\phi_{GMBt/clay}$ = 20° (peak value) $\phi_{GMBs/clay}$ = 12° (residual value)
Geogrid (GR)	$K_{t,GR}$= 1100 kN/m	/		/

In both configurations, the stability analysis at the interfaces according to limit equilibrium method is satisfied. In solution A, as the interface friction angle between the geomembrane and the clay ($\phi_{GMBs/clay}$) is lower than the slope inclination β a geogrid is used to provide the required tensile strength to the system. In solution B, the use of a double textured geomembrane results in interface friction angles higher than the slope inclination β.

Generally speaking the behaviour of the interfaces including geosynthetics are usually characterized by strain-softening behaviour (Blond and Elie 2006; Carbone 2014; Fox and Stark 2004). This implies that, in situ, if the residual interface friction angle is mobilized instead of the peak value, a decrease in the interface shear strength can occur. Interface friction angles can decrease due to several processes, including ageing of the polymer and/or as a consequence of installation (Giroud 2012). In particular, the loss in interface friction angle is higher for interfaces with textured geomembranes than those with smooth geomembranes (Carbone, 2014; Frost and Lee, 2001; Manheim et al. 2015; Stark et al. 1996) for example due to smoothing of asperities or to the hook and loop effect (Hebeler et al., 2005).

This study investigates the tensile load transferred to the geosynthetic layers where the residual value is mobilized at the interface. For this purpose, for both solutions in the calculation the residual interface friction angles (Table 1) between the geomembrane and clay ($\phi_{GMBs/clay}$) are considered.

2.2 Basic assumptions of the calculation

The analytical and the numerical calculations are based on Liu and Gilbert's (2005) hypothesis. Some of the most important hypothesis are listed below (see Liu and Gilbert, 2005, for further details):

- Soil and geosynthetics are considered as two different columns ;
- If the applied driving force due to the weight of the cover soil (W sinβ) exceeds the resisting force due to shear resistance at the base of the geosynthetic layer, then the soil will compress at the toe of the slope producing a compression force in the soil (C_{soil}) and a tension force in the geosynthetic (T_{gs});
- It is assumed that large displacement in the geosynthetics and the residual strength in the soil are mobilized;
- The slippage is not occurring at the interface between soil and geosynthetics so that the two columns strain equally;
- The soil is considered as stable and also that it is partially supported by the buttress effect at the toe of the cover layer and by tensile forces in the underlying geosynthetics. The soil buttress force acts parallel to the slope;
- The soil column is assumed to be fixed at the toe of the slope while the geosynthetic column is considered to be fixed at the anchor trench;
- The forces acting on the top and bottom of the geosynthetic layer are assumed to be uniformly distributed along the geosynthetic over the length of the cover layer. Hence, these forces can be expressed as constant shear stresses;
- The soil and geosynthetic layers are assumed to behave like elastic-plastic materials, with k_c representing the compressive stiffness of the soil and k_t representing the tensile stiffness of the geosynthetic. Non-linearity in these materials can be approximately accommodated by selecting secant stiffnesses that reflect the expected levels of deformation;
- For multiple components with the same axial behaviour (e.g. several layers of geosynthetics in tension), the distribution of load amongst multiple components can be determined by assuming equal strain in all components above the plane of slippage. Therefore, the equivalent stiffness for total compressive or tensile component of the column, K, is obtained by summing the individual stiffness values:
-

$$K = \sum_{i=1}^{n} K_i \qquad [1]$$

  where K_i is the stiffness for the i^{th} of n components in compression or tension. For an individual component, the induced load is proportional to its stiffness, relative to the total stiffness.

- The soil component does not take a compressive force that is greater than its capacity. Therefore, when the upper limit of the soil is reached, it is assumed that a plastic failure occurs and the soil column cannot take any additional load. The maximum possible tensile load in a geosynthetic component is its ultimate strength, T_{ult}.
- The geosynthetic tension increases with an increase in the stiffness of the geosynthetic relative to that of the soil: that is, an increase of K_t/K_c;
- The net applied shear stress, ϕ_{net}, is assumed to distribute uniformly along the geosynthetic layer over the length of the cover layer.

Additional hypothesis:

- The cover soil is stable and the layer is placed up in a single lift along the entire slope without any buttressing. The values found correspond to the upper bound value of the tensile force acting on the layers.
- The effect of seepage is not considered.

The equivalent axial stiffness (k_c) of 485 kN/m (Table 1) selected for the granular soil drainage layer is taken from Liu and Gilbert (2005) and based on Villard et al. (1999).

3. ANALYTICAL METHOD: LIU AND GILBERT (2005) MODEL

3.1 Input parameters and results

If the applied driving force due to the weight of the cover soil ($W \cdot \sin \beta$) exceeds the resisting force, a net applied shear force along the geosynthetic layer over the length of the soil (L_{es}) is induced. The net applied shear stress, ϕ_{net}, is assumed to distribute uniformly along the geosynthetic layer over the length of the cover layer. The forces acting on the top and bottom of the geosynthetic layer are assumed to be uniformly distributed along the geosynthetics over the length of the cover layer (hence, these forces can be expressed as constant shear stresses).
The procedure followed to calculate the total tensile load T_{gs} transferred in the geosynthetics in both solutions A and B is summarised in Figure 2.

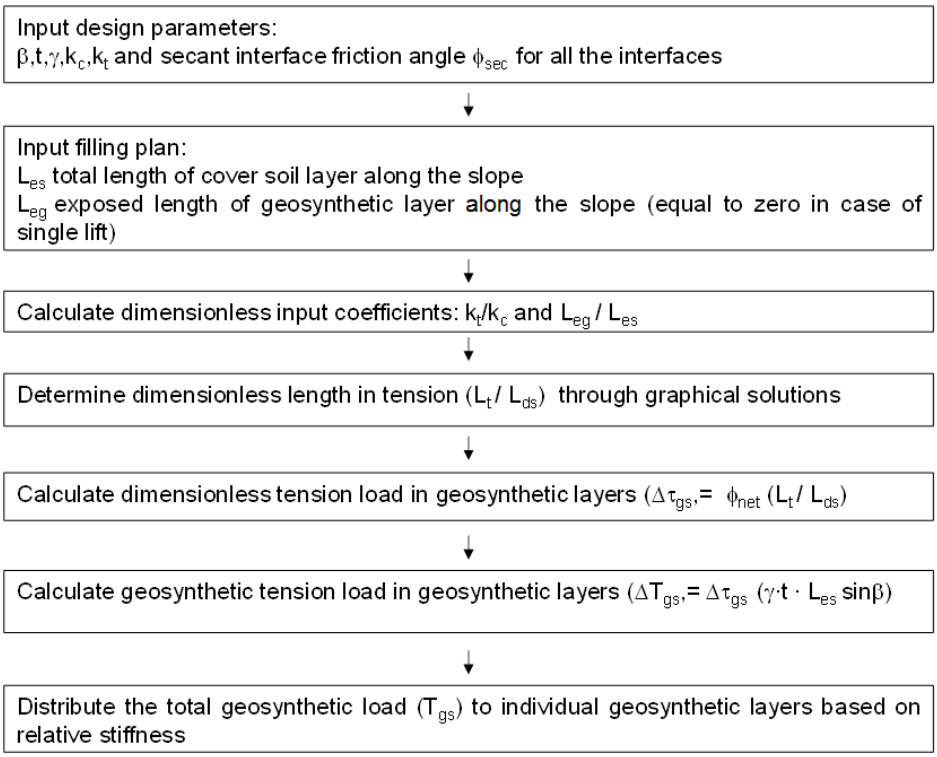

Figure 2. Procedure for estimating geosynthetic tension (modified from Liu and Gilbert 2005).

In this paper, the tension induced in the geomembranes (i.e. smooth and textured) is calculated by considering a decrease in the interface friction angle with respect to the design value. Therefore, for both systems, the critical interface friction angle $\phi_{GMB/clay}$ is chosen to be equal to 11° and 12° in solution A and B respectively (Table 1). The calculation of the tensile loads induced in the geosynthetics in both solutions are summarized in Table 2 while the graphical solutions used are shown in Figure 3.

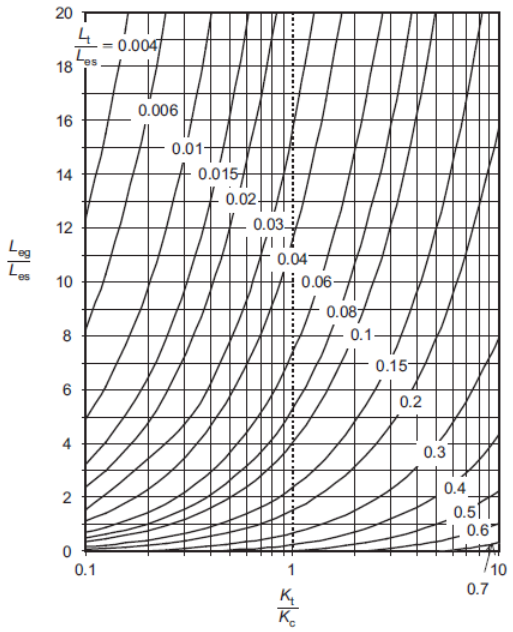

Figure 3. Graphical solution of Liu and Gilbert, (2005): length in tension, L_t/L_{es} against stiffness in ratio K_t/K_c and ratio of exposed length of geosynthetic layer to exposed length of placed cover soil layer, L_{eg}/L_{es} (adopted from Liu and Gilbert, 2005).

The results show that:

- In Solution A, the use of the geogrid not only stabilizes the system but also reduces the tensile load carried by the geomembrane.
- The use of a textured geomembrane allows a better interaction and therefore enables to reach higher slope inclinations. However, if the actual interface friction angle decreases with respect to the design value (for example due to installation damage) and it is lower than the slope inclination angle, the geomembrane will be subjected to tensile load and will carry the majority (86%) of that tensile load, ΔT_{gs} (Solution B).
- The total tensile load ΔT_{gs} in solution A is higher than the one generated in solution B because the first system is stiffer. Even so, the geomembrane will be subjected to double the tensile strength value in solution B compared to solution A.
-
-

Table 2. Tensile load transferred into geosynthetic layers applying Liu and Gilbert (2005) method.

Solution A - Smooth geomembrane system	**Solution B – Textured geomembrane system**
L_{es} = 30m; L_{eg} = 0m (one single lift)	L_{es} = 30m; L_{eg} = 0m (one single lift)
K_t= 1424.61 kN/m	K_t= 290 kN/m
K_t/ K_c= 2.94; L_t/ L_{es} =0.61	K_t/ K_c=0.6 ; L_t/ L_{es} =0.4
ϕ_{net}=0.27	ϕ_{net}=0.21
$\Delta\tau_{gs}$=0.17	$\Delta\tau_{gs}$=0.08
ΔT_{gs}=16.4 kN/m	ΔT_{gs}= 8.1 kN/m
Tensile load carried by every single layer:	Tensile load carried by every single layer:
GTX: 2.8 %	GTX: 13.8%
GMB: 19.98 %	GMB: 86.2%
GR: 77.22 %	

4. NUMERICAL ANALYSIS

In order to evaluate the behaviour of the system, a series of finite element analyses have been conducted by the use of PLAXIS code. In the numerical model, the geometry of the landfill system such as length of the geocomposite liner (L_{es}) and slope inclination (β) as well as the material properties of soil, geocomposite components (geogrid, geotextile, geomembrane) and interfaces are assumed to be identical with that formerly presented in Table 1.

To simulate the different reinforcement layers within the geocomposite liner, and the contact between them, two different scenarios have been taken into consideration: (a) all layers act together and accordingly the whole geosynthetic liner is simulated in a single structural element, while the stiffness of this element is equal to the sum of the stiffness of the different layers; (b) the geotextile and geogrid layers have good contact properties and it is likely that they will slide on the geomembrane. This latter scenario was carried out in order to verify if the distribution of the tensile loads between the different layers in geosynthetic liners is directly linearly related to their stiffness. Therefore, a very thin 'dummy layer' (thickness of 1 cm) with high stiffness has been adopted between the geomembrane and geotextile/geogrid layers within the geosynthetic lining system. The 'dummy' layer between the geotextile-geogrid and geomembrane layers can accurately simulate the contact between different layers, whilst the numerical obstacles in simulating two overleaping structural elements with the possibility of sliding is overcome. To restrict the deformations in the 'dummy' layer in the elastic domain (before sliding occurs between layers), a high elastic stiffness of 20 MPa has been assigned to it. However, to simulate the possibility of sliding occurrence above the shear resistance of the contact, the elastic-perfect plastic Mohr-Coulomb criterion has been adopted to the 'dummy' layer.

In the numerical simulations, the clay base soil beneath the geosynthetic liner is assumed to have high stiffness and therefore it will not significantly deform due to surcharge. However, the stiffness of the granular top soil is assumed to be identical to that shown in Table 1.

As shown in Table 1, the interface shear resistance in solution A or B depends on the frictional properties of the smooth or textured geomembrane. In the numerical model, the friction angle of the contact between the geotextile and geomembrane layer (in 'dummy' layer) for different solutions is defined based on the $\phi_{GTX/GMB}$ as shown in Table 1.

In both scenarios (a) and (b), the contact between the top face of the geosynthetic liner is governed by the contact properties of geogrid and granular soil while the properties of contact of the geosynthetic liner with the clay subsoil is defined based on the interface friction angle between the clay and geomembrane. These upper and lower contact surfaces have been numerically simulated by the use of interface elements between the geosyntetic layers and soil elements. It is to be noted that in scenario (a), the distribution of the load between layers is assumed to be in accordance with the stiffness of the layers while scenario (b) determines the exact value of the force that is developed in the geomembrane as well as either (geogrid-geotextile) compound element (solution A) or geotextile element (solution B).

Since the present numerical analysis is aimed at validating the analytical solution offered by Liu and Gilbert (2005), the mechanical behaviour of the material and the boundary conditions in numerical simulations are simplified to be consistent with what has been assumed within the analytical approach. For instance, the mechanical behaviour of the soil and geosyntetic layers (e.g. geotextile, geomembrane, geogrid) are assumed to be linear elastic while the properties of the contact between different materials are simulated by the use of Mohr-Coulomb constitutive model.

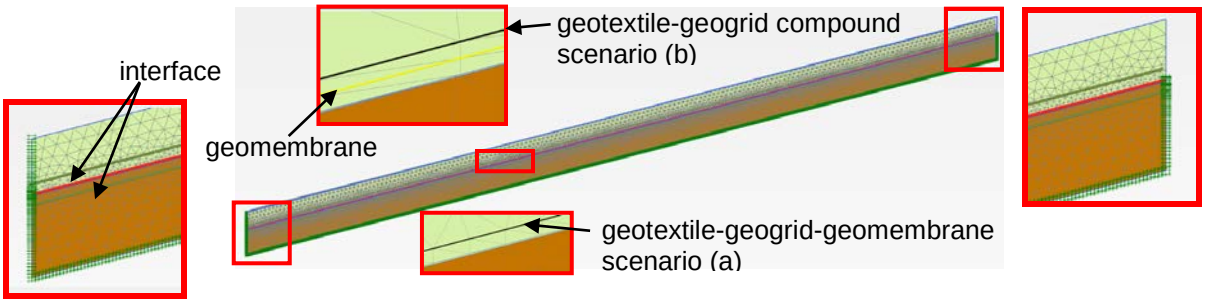

Figure 4. The schematic shape and the boundary conditions in numerical model

The schematic shape of the numerical model and the boundary conditions at the top and bottom of the model including the detail of arrangement of the layers are shown in Figure 4.

To exclude the deformations due to the weight of the system from the numerical results, the initial conditions of the model has been applied in the first stage of analysis and the corresponding deformations have been reset to zero in the second stage. In both stages, all boundaries are mechanically fixed. In the 3rd stage of simulation, the horizontal and vertical fixities of the soil on the upper part of the model are deactivated where

the geocomposite is still fixed. Accordingly, the layer of granular soil tends to be compressed towards the lower parts of the model and that generates tension in the geosynthetic layers.

According to Table 1, the friction angle between the geomembrane and the clay can be characterized by its peak or residual values. However, this study only considers the case where the friction angle of the critical interface is equal to its residual value.

Table 3. Tensile load transferred into geosynthetic layers by numerical method

	Solution A - Smooth geomembrane system	**Solution B – Textured geomembrane system**
scenario (a)	ΔT_{gs}=11,59 kN/m GTX: 1.7 % → 0,20 kN/m GMB: 18,1 % → 2,1 kN/m GR: 80,2 % → 9,29 kN/m	ΔT_{gs}=5.18 kN/m GTX: 9 % → 0,47 kN/m GMB: 91 % → 4.71 kN/m
scenario (b)	ΔT_{gs}=12 kN/m GTX+GR: 9,73 kN/m GMB: 2,27 kN/m GTX+GR: 81.1 % GMB: 18.9 %	ΔT_{gs}=5.04 kN/m GTX: 0,98 kN/m GMB: 2,27 kN/m GTX: 19 % GMB: 81 %

As seen in Table 3, the forces in different layers obtained from numerical simulation based on scenarios (a) and (b) are in very good agreement. It means, since the frictional resistance between geogrid and geotextile is much more than the contact friction angle between geomembrane and clay subsoil, the stability of the system is governed by $\phi_{GMBs/clay}$ and therefore, assuming a single compound layer consisting of geogrid and geotextile does not significantly influence the forces in the geocomposite layer. Furthermore, the good agreement between the forces obtained from the FEM method with those acquired from the analytical solution proposed by Liu and Gilbert (2005), reveals that for the selected material, the deformability of the granular upper soil plays no significant role in the determination of the forces in the geocomposite liner. Although the deformability of the clay base soil is neglected in present study, it can also play a considerable role in the development of forces within the geosynthetic layers.

To better explain the system behaviour and to evaluate the mode of deformation and failure, the shape of the deformed system, plastic points and compression/extension zone has been shown in Figure 5.

According to Figure 5 (a), the upper soil has the tendency to flow toward the lower part of the slope. It consistently fits to assumptions made by Liu and Gilbert (2005). However, the analytical solution neglects the variation of the thickness in the upper soil layer. As shown, the thickness of the granular upper soil layer has increased at the lower point of the slope while at the upper points, the thickness of deformed layer is smaller than the initial one.

Figure 5 (b) shows the geosynthetic liner consisting of geotextile-geogrid (black line) and geomembrane (red line) where the sliding zone is highlighted by solid red squares. As seen in Figure 5 (b), the ultimate shear strength is mobilized at the contact between the geomembrane and the base soil. In other words, the sliding first occurs at the contact between the geomembrane and the clay soil which has the lowest shear resistance. This is in agreement with both engineering judgment as well as the mechanisms assumed by Liu and Gilbert (2005).

Figure 5 (c) demonstrates the shape of the compression and extension zone. As seen, despite of the analytical solution that assumes the entire top layer is subjected to compression, only the lower half of the top soil layer is in compression. This means it might be more practical to use different stiffnesses for soil subjected to extension and compression. In addition, due to having these two different zones, the distribution of the force in the reinforcement layers are not uniform. Such force distribution is in contrast with the assumptions made in the analytical solution by Liu and Gilbert (2005). Regarding the fixities applied as boundary conditions to the upper soil layer and the geosynthetic liner, it can be expected that the distribution of the force in the geosynthetic layers is not uniform while the highest loads can will be developed in the

zone where the soil is under extension. The distribution of the force in the geosynthetic liner is shown in Figure 6.

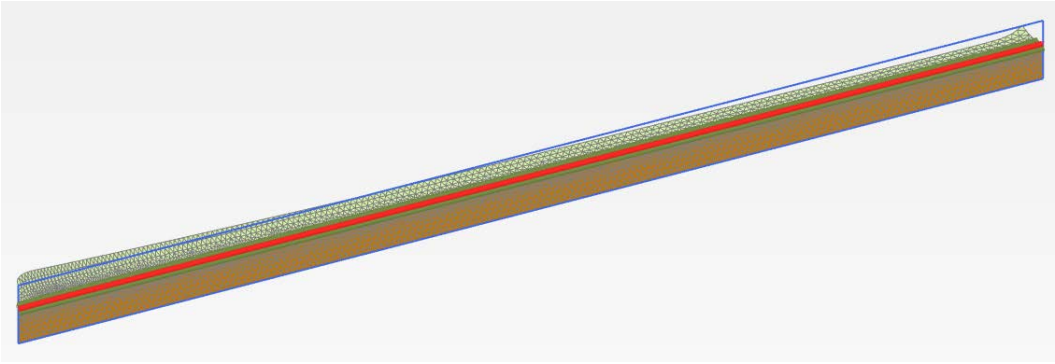

(a) deformation in the system

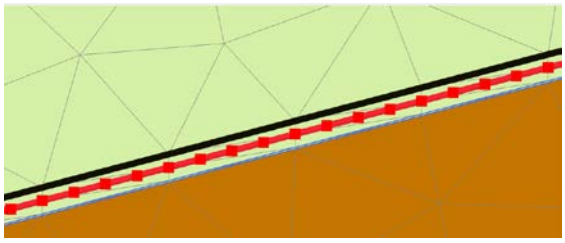

(b) plastic (sliding) points

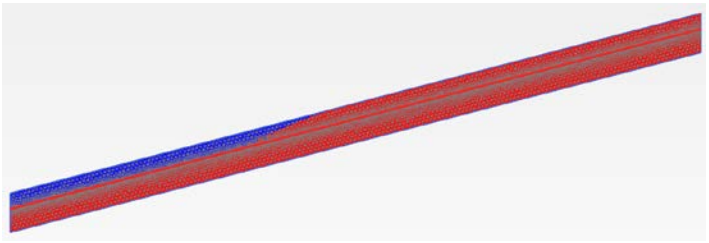

(c) compression (blue) and extension (red) zones

Figure 5. The model responses obtained from numerical analysis

As seen in Figure 6, the distribution of the force in the geosynthetic layer is not uniform. That can be the main reason for the difference in the forces obtained from the numerical solution compared to the analytical approach, which assumes the uniform force distribution in the geosynthetic liner.

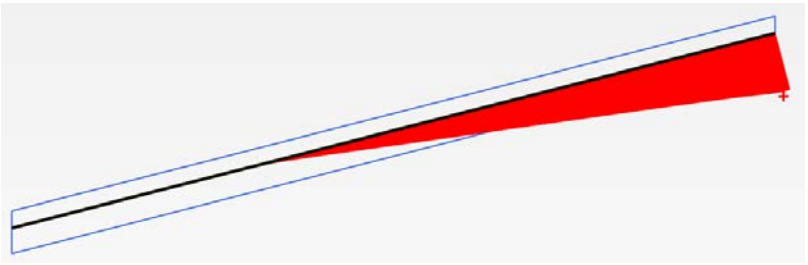

Figure 6. The schematic distribution of force in geosynthetic liner

5. CONCLUSIONS

For designing geosynthetic systems on slopes (i.e., landfill lateral barriers or cover systems), particular attention should be paid to the possible tensile loads transferred to the geosynthetic layers, especially when a geomembrane is used for sealing.
In this paper, the assessment of tension forces induced into two different geosynthetic liner configurations including a smooth and a double-faced textured geomembrane is carried out by applying a simplified analytical method based on graphical solutions (Liu and Gilbert 2005). In addition, a series of finite element numerical analyses have also been performed, to in order to validate the analytical method.

The results highlighted that for Solution A, the use of the geogrid not only stabilizes the system but also reduces the tensile load carried by the geomembrane. The use of a textured geomembrane allows a better interaction and therefore enables to reach higher slope inclinations. However, if the actual interface friction angle decreases with respect to the design value (for example due to installation damage) and it is lower than the slope inclination angle, the geomembrane will carry the majority of the tensile load (Solution B). A possible solution for this case is an appropriate geogrid reinforcement, which can be placed in the system, with the resulting tensile load carried by the textured geomembrane reduced by half.

Therefore, the following main conclusions can be drawn:

- The forces calculated by analytical and numerical analyses are in good agreement.
- The difference between the total tensile load ΔT_{gs} in analytical and numerical analyses can be related to: (a) the soil behaviour assumption considering the compression along the entire upper layer in the analytical model while the numerical results show that an extension/compression behaviour takes place; (b) the distribution of the tensile load on the geosynthetic liner is not uniform as assumed within the analytical solution.
- Based on the numerical results of scenario (b) it is demonstrated that distributing the total load with respect to the stiffness of the layers (as assumed in the Liu and Gilbert 2005 model) is realistic.

REFERENCES

Blond, E., Elie, G., (2006). Interface shear-strength properties of textured polyethylene geomembranes, in: *Sea to Sky Geotechnique 2006*, 898–904.

Carbone, L., (2014). Interface behaviour of geosynthetics in landfill cover systems under static and seismic loading conditions. Ph.D. Dissertation. Mediterranea University of Reggio Calabria and University of Grenoble, 215 pp.

Frost, J.D., Lee, S.W., (2001). Microscale study of geomembrane - geotextile interactions. *Geosynthetics International* 8, 577–597.

Fox, P. J., and Stark, T.D. (2004). State of the art report: GCL shear strength and its measurement, *Geosynthetics International*, 11(3): 141-175.

Giroud, J.P., (2012). Geosynthetics: a remarkable discipline with great achievements in the past and exciting challenges for a bright future, in: Proceedings Keynote Lecture & Educational Session, *5th European Geosynthetics Congress*. Valencia 2012 Geosynthetics, 25 – 28.

Hebeler, G., Frost, J., Myers, A, (2005). Quantifying hook and loop interaction in textured geomembrane-geotextile systems. *Geotextiles and Geomembranes* 23, 77–105.

Jones, D.R. V., Dixon, N., (1998). Shear strength properties of geomembrane/geotextile interfaces. *Geotextiles and Geomembranes* 16, 45–71.

Liu, C.-N. & Gilbert, R. B. (2003). Simplified method for estimating geosynthetic loads in landfill liner side slopes during filling. *Geosynthetics International*, 10, No. 1, 24–33

Liu, C-N. & Gilbert, R. B. (2005). Graphical solutions for estimating geosynthetic loads in geosynthetic–soil layered systems on slopes. *Geosynthetics International*, 12, No. 4,208–214.

Manheim, D.C., Yesiller, N., Hanson, J.L., Gourc, J.P., Carbone, L., Moraci, N., Carrubba, P., Pavanello, P. (2015). Investigation of Post-Shear Surface Texture Characteristics of Geomembranes. *Geosynthetics 2015* February 15-18, Portland, Oregon.

Stark, T., Williamson, T., Eid, H., (1996). HDPE geomembrane/geotextile interface shear strength. *Journal of Geotechnical Engineering*, ASCE 122 (3), 197–203.

Rowe, R.K., (2005). Long-term performance of contaminant barrier systems. *Geotechnique* 55 (9), 631–678.

Thusyanthan, N. I., Madabhushi, S. P. G., Singh S., (2007). Tension in geomembranes on landfill slopes under static and earthquake loading – centrifuge study. *Geotextiles and Geomembranes*, 25, 78-95.

Villard, P., Gourc, J. P. & Feki, N. (1999). Analysis of geosynthetic lining systems (GLS) undergoing large deformations. *Geotextiles and Geomembranes*, 17, 17–32.